



An EPR study of the two-dimensional magnetic solitons
by Kala Subbaraman

A dissertation submitted in partial fulfillment of the requirements for the degree of Doctor of
Philosophy in Physics
Montana State University
© Copyright by Kala Subbaraman (1996)

Abstract:

Two dimensional or layered Heisenberg magnets in the classical continuum limit are known to support localized regions of magnetization called solitons. A theoretical and experimental investigation of a two dimensional spin five-halves, Heisenberg antiferromagnet has been conducted. Theoretical calculations that determine how the solitons will affect the temperature-dependent electron paramagnetic resonance (EPR) linewidth have been done. These calculations include the dependence of EPR linewidth on the nonmagnetic impurity concentration. The calculation consists of two parts. The first is the determination of the discrete core energy using simple numerical methods and the energy of the continuum area surrounding the core of the soliton. The second part involves the calculation of the dynamic correlation function performed within the framework of the soliton-magnon interaction picture. One of the most significant effects indicated by the above calculations is the large change in the EPR linewidth with very small amounts of doping nonmagnetic impurity atoms. The magnon contribution to the temperature dependent linewidth was calculated by extending the calculations of Chakravarty and Orbach for a quantum Heisenberg antiferromagnet. It was found to be rather insignificant when compared to the soliton contribution in the same temperature range.

We have investigated the possible effects of doping $(n\text{-propylammonium})_2\text{Mn}_{1-x}\text{M}_x\text{Cl}_4$, a quasi two-dimensional antiferromagnet with $S = 5/2$, where $M = \text{Cadmium, Zinc or Magnesium}$. The nonmagnetic impurities are present in very small molar quantities well below the percolation limit. Very good qualitative agreement between the observed linewidth temperature dependence and the above theory indicate that solitons indeed contribute to the thermodynamic behavior of layered magnetic compounds. A quantitative comparison of the soliton excitation energies as a function of impurity concentration reveals good agreement between theory and experiment.

AN EPR STUDY OF THE TWO-DIMENSIONAL MAGNETIC
SOLITONS

by
Kala Subbaraman

A dissertation submitted in partial fulfillment
of the requirements for the degree

of

Doctor of Philosophy

in

Physics

MONTANA STATE UNIVERSITY
Bozeman, Montana
October 1996

D378
Su 139

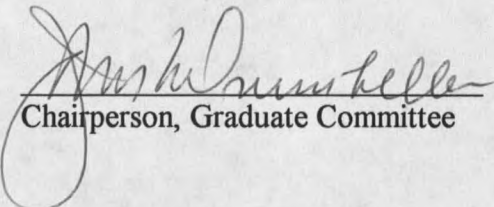
APPROVAL

of a thesis submitted by

Kala Subbaraman

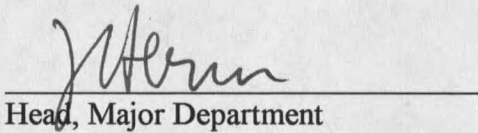
This thesis has been read by each member of the thesis committee and has been found to be satisfactory regarding content, English usage, format, citations, bibliographic style, and consistency, and is ready for submission to the College of Graduate Studies.

11/15/96
Date


Chairperson, Graduate Committee

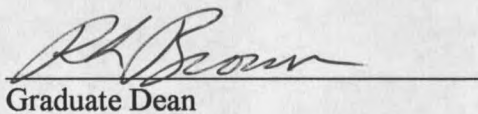
Approved for the Major Department

11-15-96
Date


Head, Major Department

Approved for the college of graduate studies

1/20/97
Date


Graduate Dean

STATEMENT OF PERMISSION TO USE

In presenting this thesis in partial fulfillment of the requirements for a doctoral degree at Montana State University, I agree that the Library shall make it available to borrowers under rules of the Library. I further agree that copying of this thesis is allowable only for scholarly purposes, consistent with 'fair use' as prescribed in the U.S. Copyright Law. Requests for extensive copying or reproduction of this thesis should be referred to University Microfilms International, 300 North Zeeb Road, Ann Arbor, Michigan 48106, to whom I have granted "the exclusive right to reproduce and distribute my dissertation for sale in and from microfilm or electronic format, along with the right to reproduce and distribute my abstract in any format in whole or in part."

Signature Stale

Date 11-16-96

ACKNOWLEDGEMENTS

I would like to sincerely thank my advisor Jack Drumheller for his support, advice, and encouragement during the time this thesis work was done. Craig Zaspel provided me with the thesis problem and helped me through nearly all aspects of it; I am indebted to Craig for sharing his ideas with me and for so much technical guidance that was given freely.

Thanks to Daniel Teske who helped me learn to use the AC susceptometer and Todd Grigereit for EPR spectrometer counsel, to Bob Parker for endless technical support on computer software and hardware issues, to Norm Williams and Erik Andersen for technical help. I wish to thank Dr. Ken Emerson for giving me free use of his chemistry laboratory and for sharing his expertise in crystal growth techniques. I am grateful to Jim Anderson for helping me with powder X-Ray diffraction measurements. Special thanks to Ray Larsen who put in lots of time and effort in the single crystal X-Ray diffraction measurements. Special appreciation is due to the office staff of Rose Waldon, Margaret Jarrett, Deb Chard and Carolyn Mazzatti who were very helpful. I thank John Hermanson for giving me the opportunity to continue my graduate studies at Montana State University and the rest of the faculty who made my stay here such an enjoyable and intellectually rewarding experience.

My husband Sunil deserves my deepest appreciation for his patience and for his constant support and encouragement during all my years at graduate school.

TABLE OF CONTENTS

	Page
1. INTRODUCTION	1
1.1 Heitler London Model theory of Hydrogen molecule	2
1.2 Magnetic order	6
1.3 Long range order in low-dimensional systems	8
1.4 Topological excitations	13
References cited in Chapter 1	18
2. SURVEY OF THE THEORY OF EPR	20
2.1 Relaxation function and dynamic susceptibility	20
2.2 Paramagnetic resonance	23
2.3 The Kubo Tomita theory of magnetic resonance	27
2.4 Correlation function of the exchange modulation	28
2.5 Spin diffusion	31
2.6 EPR lineshape studies	34
2.7 Temperature dependence of the linewidth of a 2d AFM	36
References cited in Chapter 2	38
3. SOLITON CONTRIBUTION TO THE EPR LINEWIDTH	39
3.1 Introduction	39
3.2 Solitons in 2d Heisenberg magnets	42
3.2.1 Solitons in 2d Antiferromagnets	45
3.2.2 Motivation for the current work	46
3.2.3 Effects of doping with impurities	48
3.2.4 Discreteness of the lattice	49
3.2.5 Calculation of the discrete core energy	50
3.3 EPR linewidth calculation	55
3.3.1 Soliton-Magnon interaction	56
3.3.2 Calculation of the four-spin correlation function	59
3.4 Soliton contribution to the linewidth	63
3.4.1 Calculation of $\langle \cos(\omega t) \rangle$	64
3.4.2 Calculation of $\left\langle \frac{\cos^4 \gamma}{Q^2} \right\rangle$	65
3.4.3 Calculation of the thermal averages	65
3.4.4 Calculation of the terms of the type $\langle f(\mathbf{r}_0) \rangle$	66
3.4.5 Determination of the soliton density	68

3.5 Magnon contribution to the EPR linewidth	70
References cited in Chapter 3	73
4. EPR MEASURING TECHNIQUE AND EXPERIMENTAL DETAILS	76
4.1 Introduction	76
4.1.1 Detection of magnetic resonance	76
4.1.2 Parts of a spectrometer	83
4.2 Description of the investigated sample	85
4.2.1 Crystal structure of PAMC	85
4.2.2 Crystal growth and concentration measurement	87
4.3 Anisotropy measurements	88
4.4 Linewidth measurements	96
4.5 AC susceptibility measurements	109
4.6 X-Ray diffraction measurements	112
References cited in Chapter 4	119
5. RESULTS AND DISCUSSION	121
5.1 Conclusions	135
5.2 Additional work on this problem	136
References cited in Chapter 5	138
Appendices	139
A - Discrete core energy calculation	140
B - Matlab Program	141
C - Calculation of the partition function and $\langle r_0^2 \rangle$	145

LIST OF TABLES

Table	Page
1. Summary of the anisotropy parameters for the pure and the doped samples of PAMC at $T < 65\text{K}$, obtained by fitting $(a - b \sin^2 \theta)$ to the linewidth $\Delta H(\theta)$.	90
2. Measured concentrations and excitation energies for cadmium doped compounds. Excitation energies were obtained from a linear fit to low -T EPR linewidths.	108
3. A summary of the measured concentrations and excitation energies for zinc doped compounds. Excitation energies were obtained from a linear fit to low-T EPR linewidths.	108
4. Measured concentrations and excitation energies for magnesium doped compounds. Excitation energies were obtained from a linear fit to low -T EPR linewidths.	109
5. Powder X-Ray diffraction data table for a sample of pure PAMC showing peak intensities and interplanar spacings.	116
6. Powder X-Ray diffraction data table for a sample of PAMC with some Mg showing peak intensities and interplanar spacings.	118
7. Measured and calculated excitation energies for various manganese compounds.	122
8. A comparison of the calculated soliton energies with the measured energies for cadmium doped compounds.	131
9. A comparison of the calculated soliton energies with the measured energies for zinc doped compounds.	131
10. A comparison of the calculated soliton energies with the measured energies for magnesium doped compounds.	133

LIST OF FIGURES

Figure	Page
1. Two hydrogen atoms where protons are labelled a and b and electrons are labelled 1 and 2.	3
2. (a) Antiferromagnetic order on a square lattice. (b) Bragg peaks for antiferromagnetic order on a square lattice.	6
3. Two $k = 1$ configurations. (a) $\theta = \phi$, (b) $\theta = \phi + \pi/2$.	14
4. The distribution of θ for one-dimensional solitons: (a) topological (b) nontopological solitons. From Ref 23.	16
5. An EPR absorption line.	26
6. Gaussian and Lorentzian line shapes.	27
7. 2-spin correlation functions in (a) 3-d and (b) low-d magnetic systems. The time scale is defined by the exchange frequency ω_e .	32
8. Orientation of the spin \vec{S} as a function of θ and ϕ , the polar angles.	42
9. The radial dependence of the polar angle of the spins in a 2d soliton.	43
10. The structure of a two-dimensional topological soliton in a ferromagnet.	44
11. Projection of the spins onto the square lattice at the soliton center. Small circles represent lattice sites.	51
12. A plot of the core energy vs the size parameter r_0 . The dotted line represents the curve for the soliton core energy without an impurity at the center. The solid line represents the case of a soliton with an impurity.	53
13(a). A plot of total soliton energy vs r_0 . \circ --- represents a plain soliton. \square — represents an impurity pinned soliton. (b). An expanded view of the above plot indicating the critical value of r_0 .	54
14. Diagram illustrating the relative angular separation between a magnon, a (pure) P-soliton, and an I-soliton (soliton with an impurity at the center).	59

15. Radial dependence of the structure of a soliton and a neighboring antisoliton.	67
16. Zeeman energy splitting in a magnetic field.	77
17. Lower half of the unit cell of PAMC. Only the carbon atoms of the propyl group are shown.	86
18. Angular variation of the EPR linewidth of pure PAMC at various temperatures.	91
19. Anisotropy of PAMC with some magnesium as an impurity, at various temperatures.	92
20. Anisotropy of PAMC with some cadmium as an impurity, at various temperatures.	93
21. Anisotropy of PAMC with no impurity at $T = 56.4$ K. The dotted line corresponds to the fit of equation 4.15.	94
22. Anisotropy of PAMC with some cadmium at $T = 52.5$ K. The dotted line corresponds to the fit of equation 4.15.	94
23. Anisotropy of PAMC with some magnesium at $T = 58$ K. The dotted line represents the fit of equation 4.15.	95
24. Anisotropy of PAMC with some magnesium at $T = 52$ K. The dotted line represents the fit of equation 4.15.	95
25. Linewidth temperature dependence of a 0.15% Cd doped sample.	97
26. Logarithm of the normalized linewidth vs inverse temperature for a 0.15% Cd doped sample.	98
27. Straight line fit of the logarithm of linewidth vs inverse temperature for a 0.15% Cd doped sample. The solid line is a spline interpretation.	98
28. Straight line fits to the logarithm of normalized linewidth vs T_N/T for three Cd doped compounds and PAMC yielding the soliton excitation energies as slopes. The solid line is a spline interpretation used as a guide to the eye.	99
29. Linear fits to the logarithm of the normalized linewidth vs T_N/T for four Cd doped compounds yielding the soliton excitation energies as slopes. The solid line, a spline interpretation, is a guide to the eye.	100

30. Linear fits of the logarithm of the normalized linewidth vs T_N/T for two Zn doped compounds and pure PAMC yielding the soliton excitation energies as slopes. The solid line is a spline interpretation used as a guide to the eye. 101
31. Linear fits of the logarithm of the normalized linewidth vs T_N/T for four Zn doped compounds yielding the soliton excitation energies as slopes. The solid line is a spline interpretation used as a guide to the eye. 102
32. Linear fits of the logarithm of the normalized linewidth vs T_N/T for four Zn doped compounds yielding the soliton excitation energies as slopes. The solid line is a spline interpretation serving as a guide for the eye. 103
33. Linear fits of the logarithm of the normalized linewidth vs T_N/T for three Zn doped compounds yielding the soliton excitation energies as slopes. The solid line is a guide to the eye. 104
34. Linear fits of the logarithm of the normalized linewidth vs T_N/T for three Mg doped compounds yielding the soliton excitation energies as slopes. The solid line is a guide to the eye. 105
35. Linear fits of the logarithm of the normalized linewidth vs T_N/T for three Mg doped compounds and PAMC yielding the soliton excitation energies as slopes. The solid line is a guide to the eye. 106
36. Linear fits of the logarithm of the normalized linewidth vs T_N/T for three Mg doped compounds yielding the soliton excitation energies as slopes. The solid line is a spline interpretation serving as a guide for the eye. 107
37. χ vs T data for a Mg doped sample showing a sharp transition at $(39.18 \pm 0.1)K$. An ac field of frequency 375Hz and amplitude 0.3Oe was applied. 111
38. Powder X-Ray diffraction data for a pure sample of PAMC. 115
39. Powder X-Ray diffraction data for a sample of PAMC doped with some Mg. 117
40. Predicted linewidth versus temperature depicting the contributions from both solitons and magnons in the critical region. The solid curve results from Zaspel's calculation while the dotted curve results from our calculation based on Chakravarty and Orbach's expression for the magnon contribution. 124
41. Logarithm of linewidth vs inverse temperature depicting the soliton and the magnon contributions. Both the linewidth and the temperature have been divided by appropriate units to render the ratio dimensionless. Takahashi's expression has

been used in estimating the correlation length.	125
42. Linewidth versus temperature at various impurity concentrations. Takahashi's expression for the correlation length was used in estimating the linewidth.	126
43. Predicted linewidth versus temperature. CHN's expression for the correlation length was used in estimating the linewidth.	127
44. Logarithm of linewidth versus inverse temperature in the fluctuation region. Takahashi's expression for the correlation length was assumed in the calculation of the linewidth.	128
45. Logarithm of linewidth versus inverse temperature. CHN's expression for the correlation length was used in estimating the linewidth.	129
46. Cadmium doped data compared with theory.	132
47. Zinc doped data compared with theory.	132
48. Magnesium doped data compared with theory.	133

ABSTRACT

Two dimensional or layered Heisenberg magnets in the classical continuum limit are known to support localized regions of magnetization called solitons. A theoretical and experimental investigation of a two dimensional spin five-halves, Heisenberg antiferromagnet has been conducted. Theoretical calculations that determine how the solitons will affect the temperature-dependent electron paramagnetic resonance (EPR) linewidth have been done. These calculations include the dependence of EPR linewidth on the nonmagnetic impurity concentration. The calculation consists of two parts. The first is the determination of the discrete core energy using simple numerical methods and the energy of the continuum area surrounding the core of the soliton. The second part involves the calculation of the dynamic correlation function performed within the framework of the soliton-magnon interaction picture. One of the most significant effects indicated by the above calculations is the large change in the EPR linewidth with very small amounts of doping nonmagnetic impurity atoms. The magnon contribution to the temperature dependent linewidth was calculated by extending the calculations of Chakravarty and Orbach for a quantum Heisenberg antiferromagnet. It was found to be rather insignificant when compared to the soliton contribution in the same temperature range.

We have investigated the possible effects of doping $(n\text{-propylammonium})_2\text{Mn}_{1-x}\text{M}_x\text{Cl}_4$, a quasi two-dimensional antiferromagnet with $S = 5/2$, where $M = \text{Cadmium, Zinc or Magnesium}$. The nonmagnetic impurities are present in very small molar quantities well below the percolation limit. Very good qualitative agreement between the observed linewidth temperature dependence and the above theory indicate that solitons indeed contribute to the thermodynamic behavior of layered magnetic compounds. A quantitative comparison of the soliton excitation energies as a function of impurity concentration reveals good agreement between theory and experiment.

CHAPTER 1

1. INTRODUCTION

Over the last few decades, nonlinear effects have had far reaching influence and consequences in the various branches of mathematics, physics and engineering. The idea of the nonlinear effects as a 'unifying tool' in physics is a well-established notion by now.

In the last twenty years or so, the exponential growth in soliton research^{1,2} can be attributed to the diversity of its applications and the availability of high speed computers. Soliton theory finds wide applications in some of the branches of contemporary physics such as phase transitions, statistical mechanics, quantum liquids, low-dimensional magnetism -- to name a few. Soliton-bearing systems are very popular among theorists, because of the complete integrability of the Hamiltonian systems from which they derive. During the same time soliton research was gaining ground, low dimensional magnetism has matured into a very important branch of physics. Low-d magnets serve as good model systems in solid-state physics both in theory and experiment.

The motivation for the current thesis, which constitutes an investigation of the effect of the soliton dynamics on the thermodynamics of a two-dimensional layered magnet, stems from two factors. Firstly the discovery of a series of Cu-layered oxides with extremely high superconducting transition temperature T_C , has provided a new impetus to the research activity in low-d, in particular 2d magnetism. This new class of materials, in addition to being the highest T_C superconductors, also happens to be the best models for 2d antiferromagnets (AFM). Secondly, in view of the exhaustive mathematical information available for soliton-bearing systems, they offer rare soluble

models. However experimental evidence for the existence of solitons has been slower in coming.

Insulating magnetic compounds are the most popular magnetic systems in the experimental studies of low-d magnetism. This branch of physics and solid-state chemistry has been well developed in the last twenty years or so^{3,4,5,6}. The reduced spatial dimensionality is brought about in these compounds by the insertion of large alkyl groups between magnetic chains (in the 1d case) and between layers (in the 2d case) thus limiting the atomic orbital overlap which determines the long-range order in such systems. The restricted dimensionality offers analytic tractability, thus rendering them ideal vehicles for testing theories of magnetism. In addition nature provides a large variety of compounds which can be described as quasi-low dimensional. The study of low-d magnets is important, particularly in the context of critical phenomena and second-order phase transitions. Theoretical work on the statistical mechanics of the 1d Ising chain⁷, followed by the studies of 2d Ising magnets⁸, and its various exact solutions⁹ are only a few examples which illustrate this fact. For 1d Heisenberg AFM, the exact ground state has been given by Bethe¹⁰ and has led to a whole set of exactly solvable $S = 1/2$ chain Hamiltonians.

The following is a survey of the physics relevant to the understanding of the material that will be presented in the subsequent chapters.

1.1 HEITLER-LONDON MODEL OF THE HYDROGEN MOLECULE¹¹

The simplest example for demonstrating the effective interaction between two

neutral atoms, as a function of the radial distance of separation between them, is two hydrogen atoms. The interaction Hamiltonian from such a system is given by,

$$H = H_0 + H' \quad (1.1)$$

$$H_0 = \frac{\hbar^2}{2m} (\nabla_1^2 + \nabla_2^2) - \frac{e^2}{r_1} - \frac{e^2}{r_2} \quad \text{where } m \text{ is the electron mass.}$$

The Hamiltonian H' includes the Coulomb attraction between each proton and the opposite electron and the Coulomb repulsion between the protons and the electrons.

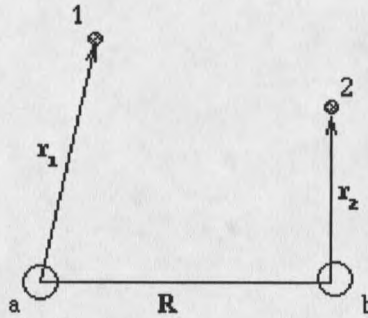


Figure. 1. Two hydrogen atoms where protons are labelled a and b and electrons are labelled 1 and 2.

$$H' = \frac{e^2}{R} + \frac{e^2}{r_{12}} - \frac{e^2}{r_{1b}} - \frac{e^2}{r_{2a}} \quad (1.2)$$

$R = |\mathbf{R}|$ is the separation between protons.

$r_{12} = |\mathbf{R} + \mathbf{r}_2 - \mathbf{r}_1|$ is the separation between the electrons.

$r_{1b} = |\mathbf{r}_1 - \mathbf{R}|$ and $r_{2a} = |\mathbf{R} + \mathbf{r}_2|$ are the separations between the electron and the opposite nuclei.

The solution to H_0 can be obtained by letting $H' = 0$, and by using a product of

hydrogen wavefunctions on the non-interacting atoms.

Let $\phi_n(\mathbf{r})$ be the eigenfunction of the single hydrogen atom with energy

$$E_n = -\frac{me^4}{2\hbar^2 n^2} \quad (1.3)$$

The eigenfunctions of H_0 are

$$\psi_p(1,2) = \phi_n(\mathbf{r}_1)\phi_m(\mathbf{r}_2),$$

$$\psi_p(2,1) = \phi_n(\mathbf{r}_2)\phi_m(\mathbf{r}_1) \quad \text{with a two-fold degeneracy.}$$

If we let the protons move closer together, the Pauli exclusion principle requires that the two electron wavefunctions be properly antisymmetrized with respect to the interchange of electrons which may be represented as,

$$\psi(\mathbf{r}_1, \mathbf{s}_1; \mathbf{r}_2, \mathbf{s}_2) = -\psi(\mathbf{r}_2, \mathbf{s}_2; \mathbf{r}_1, \mathbf{s}_1) \quad (1.4)$$

where we now explicitly include the electron spins \mathbf{s}_1 and \mathbf{s}_2 . With no spin-orbit coupling, the spin and position variables can be separated.

$$\psi(\mathbf{r}_1, \mathbf{s}_1; \mathbf{r}_2, \mathbf{s}_2) = \psi(\mathbf{r}_1, \mathbf{r}_2)\chi(\mathbf{s}_1, \mathbf{s}_2) \quad (1.5)$$

The Pauli principle requires that spin functions be antisymmetric if the spatial function is symmetric under interchange of electrons and vice versa. ψ thus has a spin singlet (s) and a spin triplet (t) part.

$$\psi_s(1, 2) = \frac{1}{\sqrt{2}} [\phi_n(\mathbf{r}_1)\phi_m(\mathbf{r}_2) + \phi_m(\mathbf{r}_1)\phi_n(\mathbf{r}_2)]\chi_s(\mathbf{s}_1, \mathbf{s}_2) \quad (1.6)$$

$$\psi_t(1, 2) = \frac{1}{\sqrt{2}} [\phi_n(\mathbf{r}_1)\phi_m(\mathbf{r}_2) - \phi_m(\mathbf{r}_1)\phi_n(\mathbf{r}_2)]\chi_t(\mathbf{s}_1, \mathbf{s}_2) \quad (1.7)$$

This particular form of the wavefunction is due to the Heitler-London approach.

It does not allow two electrons to occupy the same site and therefore has a built-in

correlation that reduces the Coulomb repulsion between electrons. In this problem, only the spin variables affect the energies of our problem. In order to estimate the singlet-triplet splitting, lowest order perturbation theory is used resulting in,

$$\Delta E_{s,t} = \frac{Q \pm J}{[1 + \beta^2]} \text{ where } \beta = \int \rho_{ab}(1) d^3 x_1 \text{ and } \rho_{ab}(1) = \phi_a^*(1)\phi_b(1),$$

and β is known as the overlap integral.

We also define charge densities of the unperturbed atomic orbitals as

$$\rho_a(1) = \phi_a^*(1)\phi_a(1) \text{ and } \rho_b(2) = \phi_b^*(2)\phi_b(2)$$

Q is defined as the *Coulomb integral* which represents the interaction between the time average charge cloud on separate unperturbed atoms. J is known as the *exchange integral* which appears as the result of the symmetry of the spatial wavefunctions under interchange of electrons they are written as,

$$Q = \frac{e^2}{R} + \int \rho_a(1) \frac{e^2}{r_{12}} \rho_b(2) d^3 x_1 d^3 x_2 - 2 \int \rho_b(2) \frac{e^2}{r_{a2}} d^3 x_2, \text{ and} \quad (1.8)$$

$$J = \int \rho_{ab}(1) \frac{e^2}{r_{12}} \rho_{ab}(2) d^3 x_1 d^3 x_2 - 2\beta \int \rho_{ab}(1) \frac{e^2}{r_{b1}} d^3 x_1. \quad (1.9)$$

Thus the interesting result from the study of molecular hydrogen is the presence of a spin-dependent interaction of a magnitude given by the electrostatic forces. The *exchange integral* J is $\approx 3 - 4$ eV in the case of hydrogen, and it arises from the symmetry requirements of the total wavefunction. Most magnetism found in nature is due to this exchange interaction.

1.2 MAGNETIC ORDER

In this section we introduce the concept of magnetic order which leads to an understanding of the systems such as a Heisenberg antiferromagnet which is the sample system studied in this work. For the simple case the spin-interaction alone can be written as,

$H_{\text{spin}} = -JS_1 \cdot S_2$ and can be generalized for all pairs of neighboring spins as

$$H_{\text{spin}} = - \sum_{i \neq j} J_{ij} S_i \cdot S_j \quad (1.10)$$

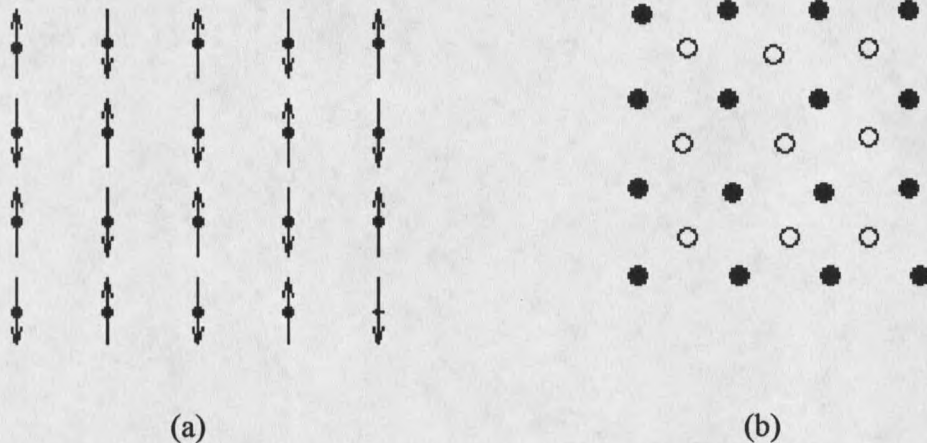


Figure 2. (a) Antiferromagnetic order on a square lattice. (b) Bragg peaks for antiferromagnetic order on a square lattice.

In magnetic materials at low enough temperatures interactions among spins lead to ordered structures, and if they prefer to be parallel, (as they do if J is positive) then a ferromagnetic phase results. If the neighboring spins prefer to be antiparallel, (when J is negative) then an antiferromagnetic phase results. The detailed form of the AFM order depends upon the lattice. On lattices, such as the square lattice in 2d that can be decomposed into two equivalent sublattices; the ordered state will consist of up spins in one

sublattice and down spins in the other. The development of AFM order leads to an increase in the size of the unit cell, and therefore, to new magnetic Bragg peaks, and a reduced size of the unit cell in reciprocal space. Furthermore in AFM an external magnetic field h does not destroy the long-range order when h is sufficiently small.

A complete description of the above mentioned ordered phases requires an introduction of a new variable quantifying the degree of order. It also requires the modification of the thermodynamics and statistical mechanics to describe the effects of these variables on free energies and entropies of the magnetic system. At low enough temperatures, even in zero magnetic field, it is possible for magnetic systems to have a spontaneous magnetization or a non-zero $\langle m \rangle$. This is the *order parameter* of a ferromagnetic state.

Depending upon the number of components, n , (x , y , z) of the spins that are considered, one has a one-, two-, or three component spin system. The number n is called the spin-dimensionality, which is distinct from the lattice dimensionality d . Depending upon the number of combinations of the components J_x , J_y , J_z there may also be a variety of models, such as Ising, XY and Heisenberg models.

The Heisenberg Hamiltonian is the same as the one represented by eqn. (1.10). It is invariant with respect to an arbitrary rotation of all the spins S_i . All the spins in the ground state of a Heisenberg Ferromagnet are along the same direction, and acquire their maximal values. The ground state of a Heisenberg Antiferromagnet has not yet been found analytically. A generalized Heisenberg model may be represented by the Hamiltonian

$$H = -2J_{\parallel} \sum_{\langle ij \rangle} S_i^z S_j^z - J_{\perp} \sum_{\langle ij \rangle} [S_i^- S_j^+ + S_i^+ S_j^-] \quad (1.11)$$

The case in which we are interested in this thesis is the isotropic, antiferromagnetic, Heisenberg model wherein, $J_{\parallel} = J_{\perp} = J < 0$. The order parameter is the staggered magnetization

$$\mathbf{N} = N_0 \hat{\mathbf{n}} \quad \text{with} \quad \hat{N}(\mathbf{x}) = \sum_i \eta_i S_i \delta(\mathbf{x} - \vec{R}_i)$$

where $\eta_i = +1$ if i is a site in sublattice A and

$$\eta_i = -1 \text{ if } i \text{ is a site in sublattice B.}$$

$S = \sum_i S_i$ commutes with H and all the three components of magnetization are conserved.

1.3 LONG RANGE ORDER IN LOW-DIMENSIONAL SYSTEMS

The concept of exchange can be extended to include interactions throughout the crystalline lattice (as opposed to nearest neighbor interactions only, as in a Heisenberg magnet). It is useful to define a pair-correlation function $C(r, T) = \frac{\langle S_0^z S_r^z \rangle}{3S(S+1)}$ to describe the thermodynamic behavior of a low-d system¹¹. We consider only the z-component of the spins for convenience. Above T_C , $C(r, T)$ decreases rapidly with increasing r , reflecting the short-range order (SRO) present in the magnetic system. As T_C is approached from above the correlation length that characterizes the degree of correlation between different spins at a particular temperature, will gradually increase until it diverges at T_C , signalling the onset of long-range order (LRO). Thus long-range

order can be understood as nonzero correlations between spins that are arbitrarily far apart. In a real time situation even though the interactions are not long range, the effects are observed over large distances. Transitions to such long-range order are characterized by both characteristic specific heat anomalies and susceptibility anomalies at the temperature T_C . Both the lattice dimensionality d and the spin-dimensionality n have a profound influence on the critical behavior of many-body systems. A question of primary importance is the presence or absence of long-range order (LRO) below some finite temperature T_C . For any value of n , 3d systems can exhibit long-range order, whereas in 1d systems a transition to LRO can occur only at absolute zero regardless of spin dimension. In the following section we shall discuss some specific examples of low- d systems which exhibit long-range order¹².

Landau's argument from a statistical standpoint, about the absence of LRO in 1d Ising chains, is quite transparent¹³. The Hamiltonian which represents a 1d Ising chain with free ends is $H_{\text{Ising}} = -2J \sum_i S_i^z S_{i+1}^z$, with the ground state energy $E = -(N-1)J$ for N spins. The reversal of a spin causes a kink in the ordered chain with an energy cost of $2J$. Since this kink may be placed in any one of the N sites, the corresponding change in entropy is $k_B \ln(N)$. Thus the free energy change due to these excitations is $\Delta F = 2J - k_B \ln(N)$ which is less than 0 for all $T > 0$ for a large enough N . The chain therefore breaks up into smaller segments or domains which minimizes the free energy, thus yielding approximately $e^{2J/k_B T}$ for the correlation length.

The correlation functions that are mentioned above are used to describe static behavior. Time-dependent correlation functions are used to describe the frequency-

dependent effects as in NMR, EPR and neutron diffraction.

The formation of domains in 1d systems, in order to minimize the free energy, indicates that short-range order (SRO) is present in magnetic systems above T_C . There are few exact solutions available for the Heisenberg model. Numerical calculations, however, are available which characterize the Heisenberg behavior to a fair degree of accuracy, particularly in 1-d^{14,15}. For a 1d Heisenberg model, the correlation length is of the form $R(T) \approx aJ/k_B T$ which has been experimentally observed for the 1d Heisenberg model TMMC¹⁶.

The important calculation for the 2d Ising model, for a $S = 1/2$ system was first done by Onsager⁸. Applying the free energy-entropy considerations to a 2d square lattice of Ising spins, the transition temperature is found to be $T_C = 2J/k_B \ln 3$. The system is stable against domain formation for $T < T_C$, but above this temperature domains will form destroying the LRO. The exact transition temperature⁸ is $T_C = 2J/k_B \ln(1 + \sqrt{2})$.

A more sophisticated version of this type of argument was first proposed by Peierls¹⁷ to prove that in a 2d Heisenberg model, phase transitions do not occur. The absence of order at any finite temperature in a 2d Heisenberg model, has been proved by Mermin and Wagner¹⁸. A 2d XY model is distinct from the other models. It has no transition to LRO in the conventional sense, i.e, a temperature below which the order parameter diverges cannot be defined; yet there exists a finite temperature at which the susceptibility diverges in an exponential fashion. According to Kosterlitz, Thouless, and Berezinskii^{19,20} this transition corresponds to the unbinding of the vortex - antivortex pairs, that exist in these systems below the ordering temperature T_{KT} .

The molecular field (MF) theory offers a remarkably good approximation to the qualitative behavior of phase transitions in 3d magnets. It, however, completely fails for low-dimensional magnets, since it fails to take into account SRO effects. In MF theory, the magnetic interaction of a given spin with its z nearest neighbors is replaced by an average interaction with all the other spins in the lattice. MF theory predicts a transition to LRO regardless of the lattice-dimensionality, which is not true for low-d systems. Even for systems that show LRO the MF theory becomes inadequate near the critical point. The fluctuations that are not accounted for in this theory become more important in models such as Ising and Heisenberg.

There will always be some weak interchain and interlayer interactions present in the experimental approximations to low-d systems that we encounter in real life. Of prime concern is, how the thermodynamic properties of these quasi low-d systems will be affected by these interactions. The 3-d order in a low-d system is basically driven by the divergence of the correlation length in the low-d system as one approaches T_C from above. The weak interchain or interlayer interactions, however small, allow correlations to propagate in three dimensions, thus allowing a 'crossover' to 3d behavior at low enough temperatures. An interesting question is whether the critical behavior close to transition merely reflects the 3d character of real layer type systems or whether it still represents specific 2d properties.

The thermodynamic behavior of low-d magnets is fundamentally different from those of their 3d counterparts because of the SRO effects that precede the onset of LRO. In order to discuss these effects it is useful to distinguish among three

temperature regimes. (a) When $T \gg T_C$, the magnetic systems are marked by random thermal fluctuations and precise estimates of the 'low-d' critical properties can be obtained. (b) The temperature region immediately above T_C is termed the fluctuation or critical regime which is determined by n , d and the strengths of the exchange constants. This region may be further subdivided into a SRO region for the higher temperature and the crossover region where 3d effects begin to arise. Effects of SRO on the temperature dependence of the spin-correlations in the critical region of a 2d layered magnet will be the focus of the current work, rather than the crossover to 3d. (c) The temperature regime $T \ll T_C$, is where the system is ordered in 3d, where spin-wave type excitations dominate the thermodynamics.

From the above discussion it is evident that a molecular field approach is inadequate to describe co-operative phenomena in low-d systems. One has to resort to more realistic models such as Ising, XY, and Heisenberg. Unfortunately because of the mathematical difficulties involved, exact results for these models are not available except for the 1d case and the 2d Ising model. For 3d models our knowledge of thermodynamic behavior is based on approximation techniques, such as high temperature series expansions, scaling theory and renormalization group for critical behavior. However, in low-d systems information about the spin dynamics in the non-ordered region could be obtained. For the 2d XY and Heisenberg models it is well known that the low-amplitude excitations are spin waves. Other large amplitude fluctuations present in these systems are nonlinear excitations like kinks, solitons and skyrmions. In the following section the concept of topological excitations is introduced which is pertinent to the theory

developed in Ch. 3.

1.4 TOPOLOGICAL EXCITATIONS

In recent years the study of nonlinear excitations such as vortices and solitons has enjoyed a vivid interest among theorists as well as experimentalists. While spin waves are the simplest type of excitations found in 2d systems that play an important role in the phase transitions of these systems, the contribution of these nonlinearities, classified as 'fluctuational excitations', cannot be ignored. Quasi-order in the XY model results from spin-waves and vortices which are topological excitations confined below a certain temperature. In the Heisenberg model vortices are prohibited; however, another type of topological excitation called a 'soliton' is allowed. This section is devoted to a discussion of these defects in magnetic systems.

Topological excitations are defects or distortions from a ground state configuration. These distortions arise from the imposition of boundary conditions, from external fields, or from thermal fluctuations. A general description of a topological defect is as follows. It can be characterized by some core region where order is destroyed, and a far field region where an elastic variable changes slowly in space. In order to elucidate the concept of topological defects we shall consider the example of a vortex in the XY-model. The order parameter that breaks the continuous symmetry of rotations in the xy-plane is a two-dimensional vector $\langle \mathbf{s} \rangle = s(\cos\theta, \sin\theta)$ whose phase is specified by the angle θ . The spin $\langle \mathbf{s}(\mathbf{x}) \rangle = s(\cos\theta(\mathbf{x}), \sin\theta(\mathbf{x}))$ is a periodic function of $\theta(\mathbf{x})$ and it is possible to have situations in which $\mathbf{s}(\mathbf{x})$ is continuous everywhere in d-dimensional space. For

